

Extremely Hot Gas in the Most X-ray Luminous Cluster RXJ1347

Naomi Ota¹, Kouichi Murase², Tetsu Kitayama³, Eiichiro Komatsu⁴, Makoto Hattori⁵, Hiroshi Matsuo⁶, Tai Oshima⁷, Yasushi Suto⁸, and Yoshikawa⁹

¹ Tokyo University of Science, 1-3 Kagurazaka, Shinjuku, Tokyo 162-8601, Japan

² Saitama University, Shimo-Okubo 255, Sakura, Saitama 338-8570, Japan

³ Toho University, 2-2-1 Miyama, Funabashi, Chiba 274-8510, Japan

⁴ The University of Texas at Austin, 2511 Speedway, RLM 15.306, Austin, TX 78712, USA

⁵ Tohoku University, Aramaki, Aoba, Sendai 980-8578, Japan

⁶ National Astronomical Observatory of Japan, 2-21-1 Osawa, Mitaka, Tokyo 181-8588, Japan

⁷ Nobeyama Radio Observatory, Minamimaki, Minamisaku, Nagano 384-1805, Japan

⁸ The University of Tokyo, Tokyo 113-0033, Japan

⁹ Center for Computational Physics, University of Tsukuba, Tsukuba, Ibaraki 305-8577, Japan

E-mail(NO): ota@rs.kagu.tus.ac.jp

ABSTRACT

We present the results from long Suzaku observations of the most X-ray luminous galaxy cluster, RX J1347.5–1145 at $z = 0.451$. To understand the gas physics of a violent, cluster merger, we study physical properties of the hot (~ 20 keV) gas clump in the south-east region discovered previously by Sunyaev–Zel’dovich (SZ) effect observations.

With the joint analysis of the Suzaku and Chandra data, we determine the temperature of the hot gas in the south-east region to be $25.3_{-4.5}^{+6.1}$ (statistical; 90% confidence level) $\pm_{9.5}^{+6.9}$ (systematic; 90% confidence level) keV, which is in an excellent agreement with the previous joint analysis of the SZ effect in radio and the Chandra X-ray data. This is the first time that the X-ray spectroscopic observations alone have enabled a good measurement of such a high temperature gas component, because of Suzaku’s unprecedented sensitivity over the wide X-ray band. These results indicate strongly that RX J1347.5–1145 has undergone a recent, violent merger. The spectral analysis shows that the SE component is consistent with being thermal. Therefore the present result confirms the presence of the hottest thermal gas in the Universe. On the other hand, no significant non-thermal hard X-ray emission is detected and we measure the 3σ upper limit to the non-thermal flux in the 12–60 keV band, $F < 8 \times 10^{-12}$ erg s⁻¹ cm⁻². Combining this limit with the synchrotron flux of a radio mini halo in this cluster, we find a lower limit to the strength of the cluster magnetic field, such that $B > 0.007$ μ G.

KEY WORDS: galaxies: clusters: individual: RX J1347.5–1145 – galaxies: intergalactic medium – X-rays: galaxies: clusters – cosmology: observations

1. Introduction

Cluster mergers are the most energetic events in the Universe after the Big Bang and strongly affect the cluster structure and the physical properties of intracluster medium (ICM). The previous multi-wavelength observations have shown that RX J1347.5–1145 has an unusually violent merger activity, which makes this cluster an ideal target for probing the gas physics and non-thermal phenomena associated with the merger at high redshifts.

RX J1347.5–1145 is the most X-ray luminous cluster of galaxies on the sky, having the bolometric luminosity of $L_{X,\text{bol}} \sim 2 \times 10^{46}$ erg s⁻¹ and the global temperature of ~ 12 keV (e.g., Schindler et al. 1997). This cluster was classified as a cooling-flow cluster because of its centrally

peaked X-ray emission and high mass accretion rate at the center (Schindler et al. 1997; Allen et al. 02).

The most striking feature of RX J1347.5–1145 is the presence of an extremely hot, ~ 20 keV, gas clump in the south-east (SE) region. This component was first pointed out by the SZ effect observation at 150 GHz as the prominent substructure, about 20” off at its the center (Komatsu et al. 2001). Kitayama et al. (2004) performed a joint analysis of the SZ data and the Chandra X-ray data, and determined the temperature of the hot gas clump to be in excess of 20 keV, which is much higher than the average temperature of the ambient gas.

The analysis of the temperature structure in merging cluster is a powerful tool for understanding the gas

physics in extreme conditions. While X-ray spectroscopy has been used widely in this type of study, it is not easy to measure precisely the temperature of very hot ($kT \gg 10$ keV) gas.

The X-ray data from the ROSAT satellite failed to identify the hot component in the SE region. This example shows the importance of having sensitivity to high temperatures well in excess of 10 keV. The unprecedented sensitivity of the Suzaku satellite to hard X-ray emission offers a wonderful opportunity to study violent merger events. In this paper, we present an analysis of the temperature structure and non-thermal, high-energy component of the distant cluster RX J1347.5–1145 with the on-board instruments, XIS and HXD. Combined with the Chandra data, we determine the temperature of the SE clump only from the X-ray spectroscopy, and discuss its physical properties. We also constrain, for the first time, the non-thermal hard X-ray emission and estimate the magnetic-field strength in the cluster.

Throughout the paper, we adopt $\Omega_M = 0.27$, $\Omega_\Lambda = 0.73$, and $H_0 = 72 \text{ km s}^{-1} \text{ Mpc}^{-1}$. At the cluster redshift ($z = 0.451$), 1'' corresponds to 5.74 kpc.

2. Observation

Long observation of RX J1347.5–1145 were conducted on 2006 June 30 and 2006 July 15. The target was observed at the HXD nominal position. The total exposure time after data filtering was 149 ks/122 ks for XIS/HXD.

The XIS spectra were extracted from a circular region within a radius of 5' centered at the X-ray peak of the cluster emission. The background spectra were accumulated from the circular region within a 3' radius (Figure 1). The HXD spectra were accumulated from all units of the PIN diodes. The method of background subtraction is presented in §3.2..

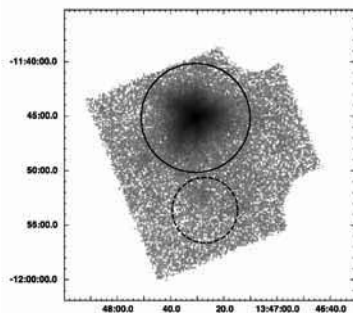


Fig. 1. Suzaku XIS-0 image of RX J1347.5–1145 in the 0.5–10 keV band. The spectral regions for the cluster and the background are indicated with the solid and dashed circles, respectively.

3. Spectral analysis and results

3.1. XIS analysis: 0.5–10 keV

To examine the global temperature structure of the cluster, we first attempted to reproduce the observed XIS spectra under the single-temperature model in two different ways: (1) by a APEC model fit, and (2) by using the intensity ratio of two Fe-K emission lines, as an indicator of the “ionization” temperature.

For the analysis (1), we fitted the APEC model to the observed 0.5–10 keV XIS spectra, where the redshift and Galactic hydrogen column density were fixed at $z = 0.451$ and $N_{\text{H}} = 4.85 \times 10^{20} \text{ cm}^{-2}$, respectively. We find the temperature, the metal abundance, and the spectral normalization factor of $kT = 12.86^{+0.08}_{-0.25}$ keV, $Z = 0.33^{+0.03}_{-0.02}$ solar, and $1.37(1.36 - 1.39) \times 10^{-2}$, respectively. The unabsorbed flux and luminosity in the 0.5–10 keV band are $F_{\text{X},0.5-10 \text{ keV}} = 1.3 \times 10^{-11} \text{ erg s}^{-1} \text{ cm}^{-2}$, and $L_{\text{X},0.5-10 \text{ keV}} = 8.7 \times 10^{45} \text{ erg s}^{-1}$, respectively.

For (2), we model the XIS spectra in the 4–5.5 keV band as the sum of (i) the APEC model with the metal abundance reset to 0 for the continuum emission and (ii) two Gaussians for the two major Fe-K lines. This model provides the line ratio, (He-like Fe $K\alpha$)/(H-like Fe $K\alpha$), of 1.05(0.92 – 1.34). Thus from temperature dependence of the line ratio predicted by the APEC model, we find $kT = 10.4(9.1 - 11.4)$ keV. This value is significantly different from that found in (1), suggesting that the ICM cannot be explained by the single-temperature model. Therefore, the ICM is more likely to be in the form of multi-temperature plasma, which we explore in §3.3..

3.2. HXD analysis: 12–60 keV

Precise modeling of the background is crucial for measuring the hard X-ray flux. For the HXD PIN diodes, the background is composed of the following three components: (i) the non-X-ray background (NXB), (ii) cosmic X-ray background (CXB), and (iii) bright point-like sources within the detector field-of-view. Of these, the NXB dominates the observed flux.

For (i), the PIN detector background was subtracted by using the NXB files provided by the HXD instrument team. We adopt the systematic error of 3% due to the uncertainty of the NXB modeling and propagate this through out our spectral analysis. For (ii), we calculated the CXB spectrum by assuming a power-law model with an exponential cut-off at 40 keV, as previously reported from the HEAO-1 A2 (Boldt 1987). For (iii), we estimated the hard X-ray flux of point sources inside the field-of-view of PIN from the XMM-Newton data of the same field and found the contribution was negligible.

We then analyzed the PIN spectra with subtracted the NXB and CXB components under the single APEC model. The temperature and normalization factor are obtained to be $kT = 20.2^{+21.4}_{-8.0} ({}^{+7.7}_{-8.7})$ keV and

$1.02^{+0.95}_{-0.43} \left({}^{+0.26}_{-0.26} \right) \times 10^{-2}$, respectively. These parameters are consistent with those derived from the XIS data. Therefore, we conclude that the hard X-ray emission observed with PIN does indeed originate in RX J1347.5–1145. The energy flux is estimated to be $3.8 \pm 0.5 (\pm 3.3) \times 10^{-12} \text{ erg s}^{-1} \text{ cm}^{-2}$ in the 12–60 keV (The first and second errors are the 1σ statistical and systematic uncertainties).

3.3. Suzaku-Chandra joint analysis

Next, we study the physical properties of the very hot component in the SE region by performing a joint analysis of the Suzaku and Chandra data. In §3.3.1., the properties of the ambient gas are derived from the spatially-resolved Chandra spectra. In §3.3.2., the spectral properties of the SE clump are derived from the Suzaku broad-band spectra combined with the Chandra data by means of a multi-temperature model. In §3.3.3., we argue that the hot component is described more accurately by thermal gas rather than non-thermal gas, and derive an upper limit to the possible non-thermal emission.

3.3.1. Modeling the cluster average component with Chandra

The deep Chandra ACIS-I data of RX J1347.5–1145 (56 ks) was analyzed to derive the average temperature profile within $5'$. The spectra for six radial bins in the north-west (NW) region, i.e., the region outside of the SE quadrant were extracted and fitted simultaneously by using the PROJCT model in the XSPEC software. Figure 2 shows the de-projected temperature profile in the NW region. We refer to the best-fit model as the “6APEC” model hereafter.

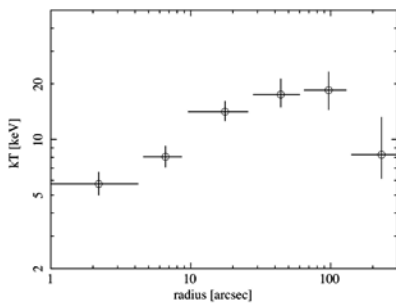


Fig. 2. Deprojected temperature profile measured from the Chandra data in the NW region.

3.3.2. Temperature measurement of the SE clump

We subtract the flux inferred by the 6APEC model (§3.3.1.) from the Suzaku data and studied the nature of the excess emission in the SE quadrant. We thus added another APEC model to describe the SE hot component to the best-fit 6APEC model and fit the Suzaku XIS

and HXD data simultaneously by the multi-temperature model (i.e., the 6APEC + APEC model). Note that because we found that the Chandra data tended to infer systematically higher values for the temperature and normalization, we took into account the systematic error coming from the uncertainty in the Suzaku-Chandra cross-calibration (See Appendix of Ota et al. 2008).

Figure 3 shows the result of joint fitting. We found the temperature of the excess emission in the SE quadrant to be $kT_{\text{ex}} = 25.3^{+6.1}_{-4.5} \left({}^{+6.9}_{-9.5} \right) \text{ keV}$, where the first error is statistical and the latter is systematic (both 90% confidence levels). The reduced χ^2 is 1315.1/1219. The absorption-corrected bolometric luminosity of the SE component is estimated as $3 \times 10^{45} \text{ erg s}^{-1}$, which is about 20% of the total luminosity.

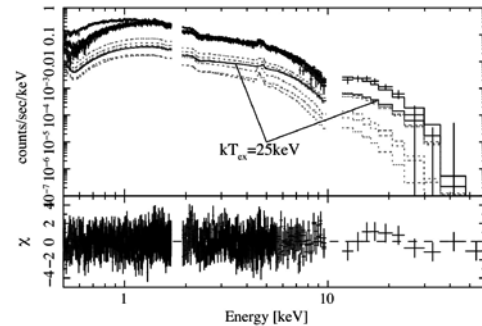


Fig. 3. 6APEC+APEC model, fit simultaneously to the observed XIS (0.5–10 keV) and HXD-PIN (12–60 keV) spectra (crosses). The gray dotted and black solid lines show the ambient component (6APEC) and the excess hot component described by an additional APEC model, respectively.

As a consistency check, we analyzed the Chandra spectrum of the SE quadrant on its own in the same manner. The best-fit temperature for the excess component is $kT_{\text{ex}}^{\text{Chandra}} = 31.1^{+24.1}_{-12.6} \text{ keV}$. Therefore, both the *Chandra*-alone analysis and the joint *Chandra*+*Suzaku* analysis implied that the excess emission had a temperature in excess of 20 keV.

Compared with the results for the *Chandra* data alone, the joint *Chandra*+*Suzaku* broad-band data analysis yielded a far more accurate determination of kT_{ex} . The *Suzaku*'s unprecedented sensitivity over the wide X-ray band made it possible to determine, for the first time, the temperature of the hot gas in the ICM solely from the X-ray spectroscopy without the help of SZ effect data.

3.3.3. Constraint on non-thermal emission

We had been assuming that the excess hard X-ray emission from the SE region is thermal; could it, however, be non-thermal? To address this question, the Suzaku data were re-analyzed in light of non-thermal emission. While

the 6APEC thermal model was again used for the ambient gas, the APEC model was replaced with a power-law (PL) model for describing the excess component.

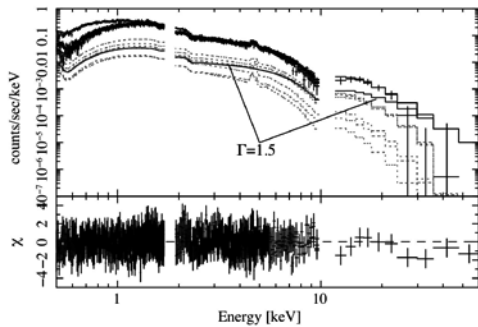


Fig. 4. 6APEC+PL model, fit simultaneously to the observed XIS and HXD-PIN spectra (crosses). The gray dotted and black solid lines show the ambient component and the excess hot component described by a non-thermal power-law model, respectively.

Figure 4 shows the results. We found that the power-law index is given by $\Gamma = 1.45^{+0.03}_{-0.04} (^{+0.09}_{-0.04})$. The reduced χ^2 of this model, $\chi^2 = 1317.1/1219$, was slightly higher than that for the thermal model.

We examined the non-thermal model more closely. In the XIS band below 10 keV, the non-thermal model with $\Gamma = 1.5$ and the thermal APEC model with 25 keV could hardly be distinguished. However, the observed PIN spectrum was far *softer* than $\Gamma = 1.5$, the effective photon index being $\Gamma_{\text{eff}} \sim 3$. When we fitted the 6APEC+PL model to the PIN data alone, the 90% lower bound on the photon index was found to be $\Gamma > 1.8$, which was significantly above the 90% upper bound on Γ from the XIS data, $\Gamma < 1.5$. Therefore, it appears difficult to explain the SE excess component with the non-thermal PL model.

4. Discussion

4.1. Properties of the extremely hot gas

From the Suzaku broad-band spectroscopy, we have found that the temperature of the SE clump is $kT_{\text{ex}} = 25.3^{+6.1}_{-4.5} (^{+6.9}_{-9.5})$ keV (90% statistical and systematic errors). This is an excellent agreement with the previous result by Kitayama et al. (2004), 28.5 ± 7.3 keV (68%; statistical only). The present result therefore confirms the presence of the hottest *thermal* gas in the cluster.

We estimate the gas density and the gas mass by simply assuming that the extremely hot gas is uniformly distributed within a sphere of $r = 25''$ (because the excess is present in $10'' < r < 60''$ of the Chandra surface brightness profile). From the measured normalization factor of the APEC model, we obtain $n_{e,\text{ex}} = (1.6 \pm$

$0.2) \times 10^{-2} \text{ cm}^{-3}$ and $M_{\text{gas,ex}} = (5.6 \pm 0.8) \times 10^{12} M_{\odot}$. We also find that the SE clump exhibits the temperature and the density that are higher than the ambient gas in the same radial bins by factors of 1.7 and 2.4, respectively. This means that the excess hot component is over-pressured, and such a region is expected to be short-lived, ~ 0.5 Gyr (Takizawa 1999). As already discussed in Kitayama et al. (2004), the gas properties can be explained by a fairly recent (within the last 0.5 Gyr or so), high velocity ($\Delta v \sim 4500 \text{ km s}^{-1}$) collision of two massive ($5 \times 10^{14} M_{\odot}$) clusters.

The heat energy of the SE clump is also estimated to be $E_{\text{th,ex}} \sim 6 \times 10^{62}$ erg. This enormous amount of energy cannot be easily produced by a central source in the cluster. On the other hand, cluster mergers, which are the most energetic events in the Universe after the Big Bang, will most naturally explain this high energy phenomenon. Therefore, our results support a merger scenario, on the basis of the X-ray spectroscopic data alone without the help of SZ data.

4.2. Estimation of the magnetic field

The non-thermal hard emission is produced via the Inverse Compton (IC) scattering of relativistic electrons off the CMB photons, and the same population of electrons also produce the synchrotron radiation. From the ratio of observed synchrotron and IC flux densities, the strength of the magnetic field can be directly estimated. We find $S_{\text{IC}} < 0.11 \mu\text{Jy}$ from our limit on the non-thermal hard X-ray emission for electrons with the IC emission frequency of $2.9 \times 10^{18} (1+z)^{-1}$ Hz. On the other hand, Gitti et al. (2007) discovered a radio mini halo in the cluster based on the VLA observations and estimated the flux density to be $S_{\text{Syn}} = 25 \text{ mJy}$ at $1.4(1+z)^{-1}$ GHz. Combining these numbers, a lower bound to the cluster magnetic-field strength is obtained as $B > 0.007 \mu\text{G}$ for the power-law index of the electron distribution $p = 2$. This limit, though weak, is consistent with typical values found in other clusters, $B \sim 0.1 - 1 \mu\text{G}$ (Rephaeli et al. 2008). However, the previous measurements were derived mostly for nearby ($z < 0.1$) clusters as well as some medium redshift clusters. Our work provides a constraint on the cluster magnetic-field strength at a higher redshift, $z = 0.451$.

References

- Allen S.W. et al. 2002 MNRAS, 335, 256
- Gitti M. et al. 2007 A&A, 472, 383
- Kitayama T. et al. 2004, PASJ, 56, 17
- Komatsu E. et al. 2001 PASJ, 53, 57
- Ota N. et al. 2008 A&A., 491, 363
- Rephaeli Y. et al. 2008, Space Science Reviews, 16
- Schindler S. et al. 1997, A&A, 317, 646
- Takizawa M. 1999, ApJ, 520, 514